Impact of Pattern Reconfigurable Antennas on Interference Alignment Over Measured Channels

Rohit Bahl[1], Nikhil Gulati[2], Kapil R. Dandekar[2], and Dwight Jaggard[1]

[1]Department of Electrical and Systems Engineering, University of Pennsylvania
[2]Department of Electrical and Computer Engineering, Drexel University,
Philadelphia, PA 19104
Email: rbahl@seas.upenn.edu, ng54@drexel.edu, dandekar@ece.drexel.edu, jaggard@seas.upenn.edu

***Abstract*—In recent years, it has been shown that concentrating interference and desired signal into separate spaces using Interference Alignment (IA), can achieve the outer bound of the degrees of freedom for the interference channel. However, the non-orthogonality of signal and interference space limits sum capacity performance. In this paper, we present the notion that by using reconfigurable antenna based pattern diversity, the optimal channel can be realized in order to maximize the distance between the two subspaces, thereby increasing sum capacity. We experimentally validate our claim and show the benefits of pattern reconfigurability using real world channels, measured in a MIMO-OFDM interference network. We quantify the results with two different reconfigurable antenna architectures. We show that an additional 47% gain in chordal distance and 45% gain in sum capacity were achieved by exploiting pattern diversity with IA. We further show that due to optimal channel selection, the performance of IA can also be improved in a low SNR regime.**

***Index Terms*—Interference Alignment (IA), reconfigurable antennas, MIMO, OFDM, channel measurements, chordal distance.**

I. Introduction

Interference management in multiuser wireless networks is a critical problem that needs to be addressed for enhancing network capacity. Cadambe and Jafar [1] made an important advancement in this direction by proving that the sum capacity of a multiuser network is not fundamentally limited by the amount of interference. In contrast with the traditional view, the number of interference free signaling dimensions, referred to as Degrees of Freedom (DoF), were shown to scale linearly with the number of users. Subsequently, they proposed Interference Alignment (IA) based precoding to achieve linear scaling of DoF and sum capacity in the high signal-to-noise ratio (SNR) regime.

The key insight for IA is that perfect signal recovery is possible if interference does not span the entire received signal space (Fig. 1). As a result, a smaller subspace free of interference can be found where desired signal can be projected while suppressing the interference to zero. Since the component of the desired signal lying in the interference space is lost after projection, the sum capacity scaling achieved comes at the expense of reduced SNR [2]. Therefore, in order to achieve optimal performance, the two spaces must be roughly orthogonal. However, as the results in [3] show, orthogonality (represented in terms of chordal distance) of the subspaces is influenced by the nature of the wireless channel and hence may not always be achievable in real world. Further, the authors provided a feasibility study of IA over measured channels and established an empirical relation between sum capacity and distance between the signal and interference space. They quantified the effect of correlated channels on the sum capacity and show the sub-optimality of IA at low SNR. Another experimental study reported in [4] showed similar degradation in the performance of IA because of practical effects such as collinearity of subspaces arising in real world channels. On the other hand, reconfigurable antennas have been shown to enhance the performance of MIMO systems by increasing the channel capacity, diversity order [5], [6] and even have been shown to perform well in the low SNR regimes, [7]. The ability of reconfigurable antennas to dynamically alter the radiation patterns and provide multiple channel realizations enable MIMO systems to adapt according to physical link conditions which leads to improved capacity. In the context of IA, reconfigurable antennas have the potential to improve its sum capacity by providing potentially uncorrelated channel realizations.

In this paper, we propose to exploit the pattern diversity offered by reconfigurable antennas to achieve an improved sub space design for IA. We experimentally evaluate the performance impact of pattern diversity on interference alignment over wideband MIMO interference channel, using three user 2×2 MIMO-OFDM channel data. The measurements were accomplished by employing two different architectures of reconfigurable antennas, which allow us to study the impact of antenna design and characteristics on the performance of IA. We provide analysis in terms of the improvements achieved in sum capacity, degrees of freedom and distance between interference and desired signal space. Through our experimental results, we show that reconfigurable antennas offer additional capacity gains in combination with IA and provide a first step in motivating the use of these antennas for enhancing interference management techniques. To the best of our knowledge, previous experimental studies on quantifying the performance of IA, limit the antenna to be omnidirectional and no experimental study has been conducted for evaluating the performance of reconfigurable antennas in networks using IA for interference management.

978-1-4673-4941-3/12/$31.00 ©2012 IEEE

Notation: We use capital bold letters to denote matrices and small bold letters for vectors. $\mathbf{H}^{-1}$, $\mathbf{H}^{\dagger}$ and $\mathbf{H}^{T}$ denote the matrix inverse, Hermitian and transpose operation respectively. Span($\mathbf{H}$), null($\mathbf{H}$) and $\|\mathbf{H}\|_F$would represent the space spanned by the columns of $\mathbf{H}$, the null space of $\mathbf{H}$ and Frobenius norm of $\mathbf{H}$ respectively. The d $\times$ d identity matrix is represented by $\mathbf{I}_d$.

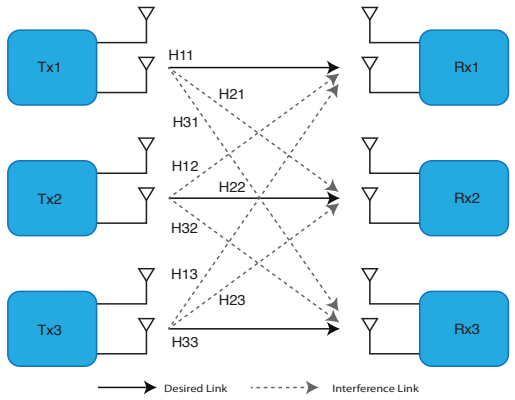

Fig. 1. Conceptual representation of the three user 2×2 MIMO interference channel.

II. System Model and Interference Alignment

Consider the K user MIMO-OFDM interference channel in which each transmitter (Tx) is equipped with M reconfigurable antennas and each receiver (Rx) is equipped with N reconfigurable antennas. The reconfigurable antennas at the transmitter and receiver have $\mathcal{P}$ and $\mathcal{Q}$ reconfigurable states respectively. Each of these states correspond to a unique radiation pattern. In such a setting, the received signal at the i^{th} receiver can then be represented by

$$\mathbf{y}^{[i]}(f) = \mathbf{H}_{q,p}^{[i,i]}(f)\mathbf{x}^{[i]}(f) + \sum_{\substack{k=1 \\ k\neq i}}^{K} \mathbf{H}_{q,p}^{[i,k]}(f)\mathbf{x}^{[k]}(f) + \mathbf{n}^{[i]}(f), \quad (1)$$

where f denotes the OFDM subcarrier index and q, p represent the antenna state selected at the receiver and transmitter respectively, $\mathbf{y}^{[i]}$ is the $N \times 1$ received column vector, $\mathbf{H}_{q,p}^{[i,k]}$ is the $N \times M$ MIMO channel between Tx k and Rx i, $\mathbf{x}^{[k]}$ is the $M \times 1$ input column vector and $\mathbf{n}$ represents the $N \times 1$ vector of complex zero mean Gaussian noise with covariance matrix $\mathbb{E}\left[\mathbf{n}\mathbf{n}^{\dagger}\right] = \sigma^2\mathbf{I}_N$. The total number of data carrying OFDM subcarriers will be represented by F_s ($F_s = 52$). For brevity, we will drop the symbols f, p and q. Here $\mathbf{x} \in \mathbb{C}^{M\times 1}$, $\mathbf{y} \in \mathbb{C}^{N\times 1}$ and $\mathbf{H} \in \mathbb{C}^{N\times M}$. The input vector $\mathbf{x}$ is subject to an average power constraint, $\mathbb{E}\left[Tr(\mathbf{x}\mathbf{x}^{\dagger})\right] = P$. Total power is assumed to be equally distributed across the input streams, i.e. the input covariance matrix $\mathbf{Q} = \frac{P}{d_k}\mathbf{I}_{d_k}$, where d_k streams are transmitted by the k^{th} transmitter. Throughout this paper, we will restrict our study to $K = 3$; $M = N = 2$ and $d_k = 1$, $\forall\ k \in \{1, 2, 3\}$. The space of all the links in the network for all the states of reconfigurable antenna will be represented by the vector $\Omega = \{i_p, j_q\}$, $i, j \in \{1, 2, 3\}$, $p \in \mathcal{P}$ and $q \in \mathcal{Q}$.

A. Interference Alignment for the 3 user, 2×2 MIMO Channel

The goal of IA is to make the signal to interference ratio (SIR) infinite at the output of each receiver. Specifically, if each transmitter transmits D independent streams of information, then to achieve perfect alignment at each receiver, dimensionality of the interference space must be restricted to $N - D$ in a $\mathbb{C}^N$ dimensional received signal space [1]. That is, there is a D dimensional subspace in $\mathbb{C}^N$ which is free of interference. The design of the precoding filters for the MIMO interference channel forces interference to exist in a smaller subspace. It has been shown that designing such precoding filters is NP hard in general for MIMO systems [8] and closed form solutions exist only for certain special cases such as the three user 2×2 MIMO channel [1].

Let $\mathbf{v}^{[i]}$ and $\mathbf{u}^{[i]}$ represent the transmit precoder and receive interference suppression filter respectively, where $i \in \{1, 2, 3\}$ and $\mathbf{v}^{[i]}$, $\mathbf{u}^{[i]} \in \mathbb{C}^{2\times 1}$. Moreover, $\mathbf{v}^{[i]}$ and $\mathbf{u}^{[i]}$ should satisfy the feasibility conditions for IA [9] given by

$$\mathbf{u}^{[i]\dagger}\mathbf{H}^{[i,j]}\mathbf{v}^{[j]} = 0, j \in \{1, 2, 3\}, j \neq i, \quad (2)$$

$$\text{rank}\left(\mathbf{u}^{[i]\dagger}\mathbf{H}^{[i,i]}\mathbf{v}^{[i]}\right) = 1. \quad (3)$$

To avoid adding any additional power in the input symbols, we restrict the norm of $\mathbf{v}^{[i]}$ and $\mathbf{u}^{[i]}$ to be 1, i.e. $\left\|\mathbf{v}^{[i]}\right\|_F$,$\left\|\mathbf{u}^{[i]}\right\|_F$ = 1.

After precoding the input symbol $x^{[i]}$ with $\mathbf{v}^{[i]}$, the signal received at the i^{th} receiver can be represented by (4). For perfect alignment at the i^{th} receiver, the interference signal vectors represented by $\mathbf{H}^{[i,k]}\mathbf{v}^{[k]}$, $k \neq i$ in (4) must span a common subspace of the received signal space. We can then express this alignment condition using the defined interference vectors as (5-7).

$$\mathbf{y}^{[i]} = \mathbf{H}^{[i,i]}\mathbf{v}^{[i]}x^{[i]} + \sum_{\substack{k=1 \\ k\neq i}}^{K} \mathbf{H}^{[i,k]}\mathbf{v}^{[k]}x^{[k]} + \mathbf{n}^{[i]} \quad (4)$$

$$\text{span}(\mathbf{H}^{[1,2]}\mathbf{v}^{[2]}) = \text{span}(\mathbf{H}^{[1,3]}\mathbf{v}^{[3]}) \quad (5)$$

$$\mathbf{H}^{[2,1]}\mathbf{v}^{[1]} = \mathbf{H}^{[2,3]}\mathbf{v}^{[3]} \quad (6)$$

$$\mathbf{H}^{[3,1]}\mathbf{v}^{[1]} = \mathbf{H}^{[3,2]}\mathbf{v}^{[2]} \quad (7)$$

Closed form solution for the alignment condition expressed in (5-7), given the feasibility constraints (2) and (3), can then be found by solving the following eigenvalue problem

$$\text{span}(\mathbf{v}^{[1]}) = \text{span}(\mathbf{E}\mathbf{v}^{[1]}) \quad (8)$$

$$\mathbf{v}^{[2]} = \mathbf{F}\mathbf{v}^{[1]} \quad (9)$$

$$\mathbf{v}^{[3]} = \mathbf{G}\mathbf{v}^{[1]} \quad (10)$$

$$\mathbf{E} = \left(\mathbf{H}^{[3,1]}\right)^{-1}\mathbf{H}^{[3,2]}\left(\mathbf{H}^{[1,2]}\right)^{-1}\mathbf{H}^{[1,3]}\left(\mathbf{H}^{[2,3]}\right)^{-1}\mathbf{H}^{[2,1]} \quad (11)$$

$$\mathbf{F} = \left(\mathbf{H}^{[3,2]}\right)^{-1}\mathbf{H}^{[3,1]} \quad (12)$$

$$\mathbf{G} = \left(\mathbf{H}^{[2,3]}\right)^{-1}\mathbf{H}^{[2,1]} \quad (13)$$

$$\mathbf{v}^{[1]} = \text{Eigenvec}(\mathbf{E}), \quad (14)$$

where the function Eigenvec($\mathbf{E}$) selects the first eigenvector of $\mathbf{E}$. The i^{th} receiver can suppress all the interference by projecting the received signal (4) on the orthogonal complement of the interference space (15) i.e., the interference suppression filter must satisfy span $\left(\mathbf{u}^{[i]}\right) = \text{null}\left([\mathbf{H}^{[i,j]}\mathbf{v}^{[j]}]^T\right)$.

$$\mathbf{u}^{[i]\dagger}\mathbf{y}^{[i]} = \mathbf{u}^{[i]\dagger}\mathbf{H}^{[i,i]}\mathbf{v}^{[i]}x^{[i]} + \sum_{\substack{k=1 \\ k\neq i}}^{K} \mathbf{u}^{[i]\dagger}\mathbf{H}^{[i,k]}\mathbf{v}^{[k]}x^{[k]} + \mathbf{u}^{[i]\dagger}\mathbf{n} \tag{15}$$

$$= \mathbf{u}^{[i]\dagger}\mathbf{H}^{[i,i]}\mathbf{v}^{[i]}x^{[i]} + \mathbf{u}^{[i]\dagger}\mathbf{n} \tag{16}$$

Note that $\mathbf{u}^{[i]\dagger}\mathbf{H}^{[i,i]}\mathbf{v}^{[i]}$ acts as the effective SISO channel between Tx/Rx pair (i, i).

III. Experimental Setup

A. Reconfigurable Circular Patch Array (RCPA)

Reconfigurable Circular Patch Arrays (RCPA) [10] are capable of dynamically changing the shape of their radiation patterns by varying the radius of a circular patch. Each antenna has two feed points and can work as a two element array in a single physical device. By simultaneously turning the switches on or off, the RCPA can generate orthogonal radiation patterns at the two ports. This provides a total of two states of operation (Mode3 and Mode4) providing two unique radiation patterns. Also, the two antenna ports have isolation higher than 20 dB. The measured radiation patterns in the azimuthal plane at the two ports of RCPA are shown in Fig. 2.

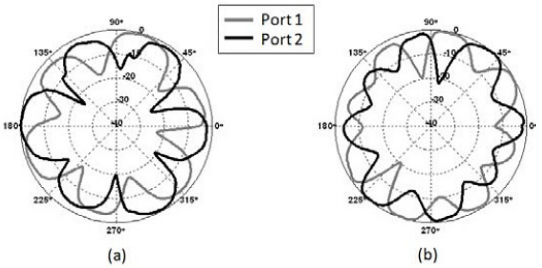

Fig. 2. RCPA Radiation Patterns (in dB) in the azimuthal plane at Port 1 and 2. a) port 1: *Mode3*, port 2: *Mode3*; b) port 1: *Mode4*, port 2: *Mode4*

B. Reconfigurable Printed Dipole Array (RPDA)

A second type of pattern reconfigurable antenna used in our experiments is the Reconfigurable Printed Dipole Arrays (RPDA) [6]. In the array configuration, RPDAs can generate multiple radiation patterns by electronically changing the length of the dipole. The radiation patterns shown in Fig. 3 are generated due the varying level of mutual coupling between the elements in the array as the geometry is changed by activating the PIN diodes to change the length of the dipole. The RPDA has four states: *short-short*, *short-long*, *long-short*, and *long-long*. In the "*short*" and the "*long*" configuration, the switch on the antenna is inactive and active respectively.

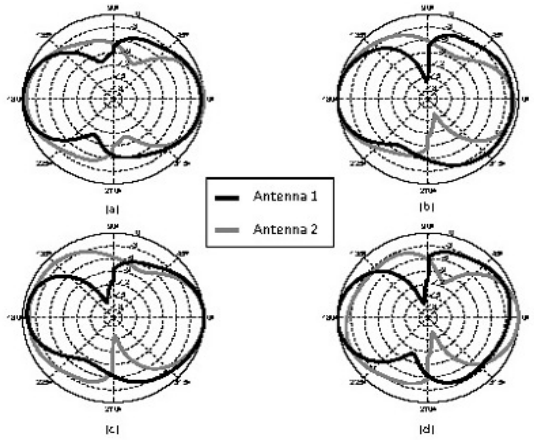

Fig. 3. RPDA Radiation Patterns (in dB) in the azimuthal plane with antenna element separation of $\lambda/4$. a) *short-short*; b) *long-short*; c) *short-long*; d) *long-long*

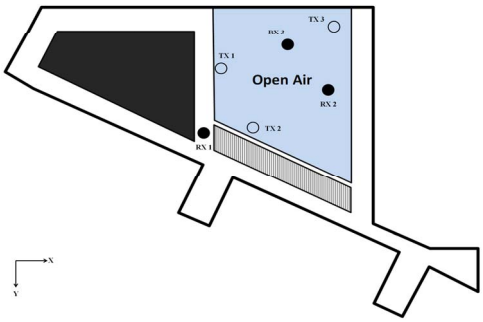

Fig. 4. 3 User 2×2 MIMO Indoor Experimental Setup

C. Measurement Setup

For channel measurements, we made use of HYDRA Software Defined Radio platform in a 2×2 MIMO setup at 2.4 GHz band using 64 OFDM subcarriers, with 52 data subcarriers. The measurements were conducted on the third floor of the Bossone Research Center in Drexel University in an indoor setup. Three designated receiver nodes and three transmitter nodes were equipped with reconfigurable antenna, with each node equipped with two antenna elements. The network topology shown in Fig. 4 was then used to activate each transmitter-receiver pair to measure the channel response and then the superposition principle was used to recreate an interference-limited network. In order to further capture the small-scale fading effects, the receiver nodes were placed on a robotic antenna positioner and were moved to 40 different positions. Receiver 1 and 2 were moved $\lambda/10$ distance along y-axis and Receiver 3 was moved $\lambda/10$ distance along x-axis. For each position and each transmitter-receiver pair, 100 channel snapshots were captured and averaged for each subcarrier. After the completion of the measurement campaign, 240 channel realizations corresponding to 40 locations and 6 network topologies were collected for each subcarrier and for each antenna configuration. This entire experiment was repeated for both RCPA and RPDA.

IV. Performance Metrics and Evaluation

A. Sum Capacity

Normalization of Channel Values: In order to calculate and compare the sum capacity results from two different set of reconfigurable antenna architectures, we proceed by forcing the most efficient states of both the antennas to receiver equal power. We also remove the effect of path loss to make sure that the capacity gains observed are solely because of the antenna characteristics [11]. To achieve this, we normalize the channels obtained from both the antennas separately with the normalization factor η, given as

$$\eta = \max_{i,j \in \Omega} \mathbb{E}\left[\sum_{f=1}^{F_s} \left\| \mathbf{H}^{[i,j]}(f) \right\|_F^2\right], \tag{17}$$

where the expectation was taken over all the 40 measurement locations. The normalized channels are then given by

$$\mathbf{H}_{normalized} = \mathbf{H}_{measured} \times \sqrt{\frac{NM \times F_s}{\eta}}. \tag{18}$$

This type of normalization effectively equates the efficiency of the most efficient state of RCPA (Mode3) to the most efficient state of RPDA (short-short). Such an approach also preserves the frequency selective nature of the wireless channel, relative difference in efficiency between states of each antenna and topology of the network.

Ergodic Sum Capacity of the network can then be approximated by [12],

$$C_\Sigma = \frac{1}{F_s} \sum_{f=1}^{F_s} \sum_{k=1}^{K} \log_2 \det(\mathbf{I}_{d_k} + \mathbf{R}^{-1[k]} \mathbf{H}_{eff}^{[k,k]} \mathbf{Q}^{[k]} \mathbf{H}_{eff}^{[k,k]\dagger}), \tag{19}$$

where,

$$\mathbf{H}_{eff}^{[k,k]} = \mathbf{u}^{[k]\dagger} \mathbf{H}^{[k,k]} \mathbf{v}^{[k]}, \tag{20}$$

represents the effective channel between k^{th} transmitter-receiver pair and

$$\mathbf{R}^{[k]} = \sigma^2 \mathbf{u}^{[k]\dagger} \mathbf{u}^{[k]} + \sum_{\substack{j=1 \\ j \neq k}}^{K} \mathbf{u}^{[k]\dagger} \mathbf{H}^{[k,j]} \mathbf{v}^{[j]} \mathbf{Q}^{[j]} \mathbf{v}^{[j]\dagger} \mathbf{H}^{[k,j]\dagger} \mathbf{u}^{[k]}, \tag{21}$$

represents the interference plus noise covariance matrix at the k^{th} receiver.

B. Chordal Distance

It is desirable to keep the signal and interference space roughly orthogonal, as interference suppression leads to the loss of signal component lying in the interference space. This reduces the projection of the desired signal in the interference space resulting in higher sum capacity. Channel realizations corresponding to different states of the antenna, results in varying degree of distance between the interference and signal space. We, therefore, use *chordal distance* (22), defined over the Grassmann manifold $\mathcal{G}(1,2)$ [13], as the distance metric to quantify performance gains:

$$d(\mathbf{X}, \mathbf{Y}) = \sqrt{\frac{c_X + c_Y}{2} - \|O(\mathbf{X})^\dagger O(\mathbf{Y})\|_F^2}, \tag{22}$$

where c_X denotes the number of columns in matrix $\mathbf{X}$ and $O(\mathbf{X})$ denotes the orthonormal basis of $\mathbf{X}$. The sum capacity performance (19) then becomes a function of the chordal distance between the two spaces. Motivated by [2], we define and use the total chordal distance across the 3 users as

$$\begin{aligned} D_{total} = {} & d(\mathbf{H}^{[1,1]}\mathbf{v}^{[1]}, \mathbf{H}^{[1,2]}\mathbf{v}^{[2]}) + d(\mathbf{H}^{[2,2]}\mathbf{v}^{[2]}, \mathbf{H}^{[2,1]}\mathbf{v}^{[1]}) \\ & + d(\mathbf{H}^{[3,3]}\mathbf{v}^{[3]}, \mathbf{H}^{[3,1]}\mathbf{v}^{[1]}). \end{aligned} \tag{23}$$

In order to find the optimal state, the channel corresponding to each of the combination of $\mathcal{P}$ reconfigurable states at the transmitter and $\mathcal{Q}$ reconfigurable states at the receiver were measured. Total chordal distance using (23) was then calculated for all the measured channels and the state q and p that maximizes the total chordal distance were selected at the receiver and the transmitter respectively.

C. Degrees of Freedom achieved

The 3 user 2×2 MIMO channel can achieve maximum of 3 DoF [1], which translates to 3 simultaneous interference free streams. We study the achieved DoF of IA with and without using reconfigurable antennas and compare the performance in Sec. V. As asymptotically high SNR is not available in practical scenarios, an approximation for DoF (24) as defined in [1], is obtained by performing regression on the SNR versus sum capacity curve.

$$DoF = \lim_{SNR \to \infty} \frac{C_\Sigma(SNR)}{\log_2(SNR)} \tag{24}$$

V. Results and Discussion

We evaluate the performance impact of the reconfigurable antennas and compare the performance of the two antenna architectures in this section. An SNR of 20 dB was maintained for all the nodes in the network which provided sufficient accuracy for the collection of channel realizations. The CDF plots were generated using 240 channel realizations collected from 40 different positions of transmitter-receiver pair and 6 different topologies of the network. We choose the most efficient operating states of RCPA and RPDA (*Mode 3* and *short-short* respectively) as the substitutes for comparison with non-reconfigurable antennas. The comparison between the two antennas is enabled by using the normalization procedure explained in Sec. IV-A.

It can be observed from the CDF of the total chordal distance for RPDA and RCPA in Fig. 5 and Fig. 6 respectively, that IA combined with using reconfigurable antennas, significantly enhances the achieved chordal distance. We highlight that RPDA out performs RCPA in terms of percentage improvement, which can be attributed to the greater number of patterns available in RPDA, improving its pattern diversity.

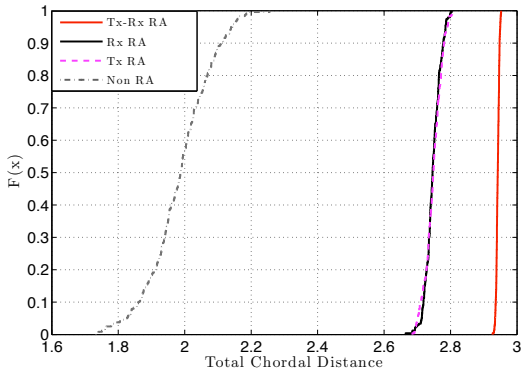

Fig. 5. CDF of the total chordal distance achieved via RPDA

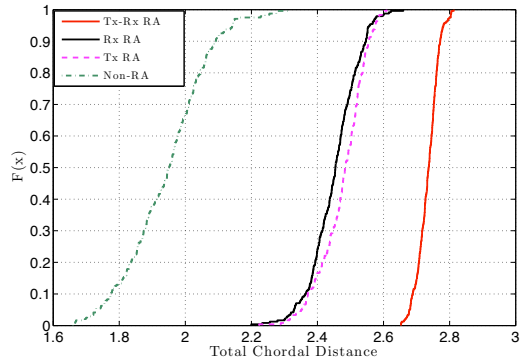

Fig. 6. CDF of the total chordal distance achieved via RCPA

Also, the percentage improvement in chordal distance is almost the same for the two scenarios when RCPA is employed at both sides of the link (transmitter-receiver) and RPDA only at one side of the link (transmitter or receiver). This equal improvement is observed because of the equal number of reconfigurable states available in the network for optimal mode selection in both the cases. Summarized results in Table I indicate that the subspaces designed via optimal selection of the antenna state can achieve close to perfect orthogonality and total chordal distance can approach the theoretical maximum value of 3.

TABLE I
MEAN VALUE OF TOTAL CHORDAL DISTANCE

	RCPA	% Increase over Non-RA	RPDA	% Increase over Non-RA
IA Non-RA	1.94	N/A	1.99	N/A
IA Tx-RX RA	2.73	40.72	2.94	47.74
IA RX RA	2.38	27.84	2.75	38.19
IA TX RA	2.45	26.29	2.75	38.19

Further, in Fig. 7 and 8 we study the impact of enhanced chordal distance on the sum capacity performance of IA. Although, we observe that adding reconfigurability enhances the sum capacity performance of IA, the gains achieved are less prominent for RCPA despite the enhanced chordal distance seen in Table I. This apparent independence of sum capacity and chordal distance performance is observed because chordal distance only exploits the underlying orthonormal space to measure distance, making it insensitive to the relative difference in the efficiency of states of the reconfigurable antennas. Since the states of RPDA have efficiency close to each other, its sum capacity performance is better than RCPA. It can be observed that, for both RPDA and RCPA, the performance of transmitter and receiver side configuration are similar since the chordal distance obtained are also quite similar. Similar performance in terms of sum capacity shows that given equal efficiency, chordal distance is closely related to sum capacity performance.

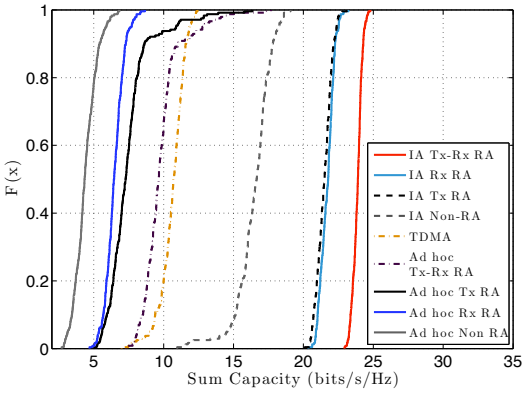

Fig. 7. Empirical CDF plot of Sum - Capacity for RPDA (SNR = 20 dB)

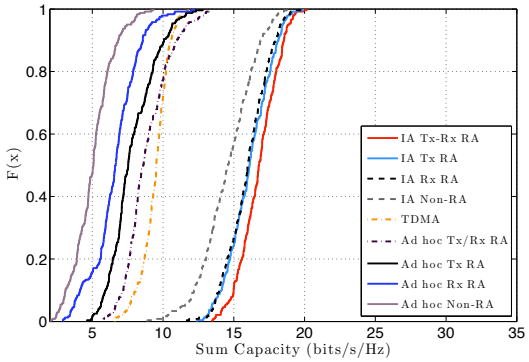

Fig. 8. Empirical CDF plot of Sum - Capacity for RCPA (SNR = 20 dB)

We observe performance gains of the order of 45 % and 15 % (at 20 dB SNR) over non-reconfigurable antennas respectively with RPDA and RCPA employed at both transmitter and receiver. We also compare IA to other transmit strategies such as TDMA, networks using no interference avoidance strategy (Ad hoc) with and without reconfigurable antennas and observe that as predicted in theory, IA outperforms them all.

In Fig. 9 and 10, we show the sum capacity in different SNR regimes. The plots illustrate that maximum sum capacity is achieved by IA with full reconfigurability at both transmitter and receiver. The marginal gains realized because of increased chordal distance are more prominent in the low SNR region since non-orthogonal spaces degrade the performance of IA in

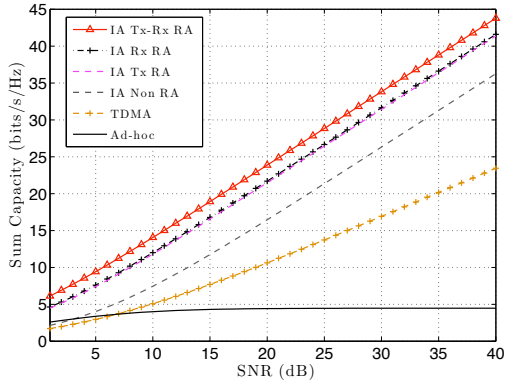

Fig. 9. Sum capacity vs. SNR for RPDA

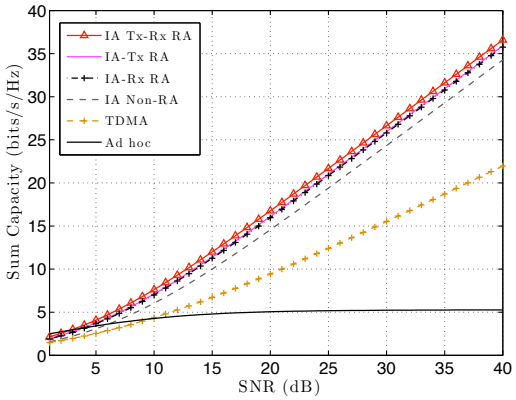

Fig. 10. Sum capacity vs. SNR for RCPA

that regime [3] [4]. As more reconfigurable states are added to the network, increasing gains in sum capacity are observed.

TABLE II
DEGREES OF FREEDOM (DOF) ACHIEVED

	RCPA	RPDA
TDMA	1.64	1.74
IA Non-RA	2.65	2.74
IA Tx-Rx-RA	2.77	2.95
TX Rx-RA	2.74	2.90
TX Tx-RA	2.73	2.90

Characterizing DoF from the slopes of the traces in Fig. 9 and 10 reveals that using IA with reconfigurable antennas can improve the achieved DoF while increasing the sum capacity at the same time. The achieved DoF are summarized in Table II. For the three user 2×2 MIMO system, a maximum of 3 DoF can be achieved. With RPDA at both transmitter and receiver we were able to achieve close to 2.94 as compared to 2.74 with non-reconfigurable structures. Additionally, it can be seen that TDMA achieved only a max of 1.74 as compared to 2.94 achieved by IA. Therefore, our measurements also show that IA performs better than TDMA under realistic channels and its performance can further be enhanced using reconfigurable antennas.

VI. CONCLUSION

In this paper, we have shown that reconfigurable antennas can significantly enhance the performance of IA by enabling an additional degree of freedom for optimal channel state selection. We quantify the effect of pattern diversity on enhanced chordal distance and the sum capacity performance of the network. Our results from measured channel data show the feasibility of using reconfigurable antennas for enhancing interference management techniques such as IA. Future work will involve further analysis to quantify the training overhead required to find the optimal antenna state. Integrating and extending existing state selection techniques [14], [10] in future is essential for real-time operation.

ACKNOWLEDGMENT

The authors wish to acknowledge John Kountouriotis, Kevin Wanuga and David Gonzalez for their valuable suggestions and feedback. This material is based upon work supported by the National Science Foundation under Grant No. 0916480.

REFERENCES

[1] V. Cadambe and S. Jafar, "Interference alignment and degrees of freedom of the-user interference channel," *Information Theory, IEEE Transactions on*, vol. 54, no. 8, pp. 3425–3441, 2008.

[2] H. Sung, S. Park, K. Lee, and I. Lee, "Linear precoder designs for K-user interference channels," *Wireless Communications, IEEE Transactions on*, vol. 9, no. 1, pp. 291–301, 2010.

[3] O. El Ayach, S. Peters, and R. Heath, "The feasibility of interference alignment over measured MIMO-OFDM channels," *Vehicular Technology, IEEE Transactions on*, vol. 59, no. 9, pp. 4309–4321, 2010.

[4] O. González, D. Ramirez, I. Santamaria, J. Garcia-Naya, and L. Castedo, "Experimental validation of interference alignment techniques using a multiuser MIMO testbed," in *Smart Antennas (WSA), 2011 International ITG Workshop on*. IEEE, 2011, pp. 1–8.

[5] J. Boerman and J. Bernhard, "Performance study of pattern reconfigurable antennas in MIMO communication systems," *Antennas and Propagation, IEEE Transactions on*, vol. 56, no. 1, pp. 231–236, 2008.

[6] D. Piazza, N. Kirsch, A. Forenza, R. Heath, and K. Dandekar, "Design and evaluation of a reconfigurable antenna array for MIMO systems," *Antennas and Propagation, IEEE Transactions on*, vol. 56, no. 3, pp. 869–881, 2008.

[7] A. Sayeed and V. Raghavan, "Maximizing MIMO capacity in sparse multipath with reconfigurable antenna arrays," *Selected Topics in Signal Processing, IEEE Journal of*, vol. 1, no. 1, pp. 156–166, 2007.

[8] M. Razaviyayn, M. Sanjabi Boroujeni, and Z. Luo, "Linear transceiver design for interference alignment: Complexity and computation," in *Signal Processing Advances in Wireless Communications (SPAWC), 2010 IEEE Eleventh International Workshop on*. IEEE, 2010, pp. 1–5.

[9] C. Yetis, T. Gou, S. Jafar, and A. Kayran, "On feasibility of interference alignment in MIMO interference networks," *Signal Processing, IEEE Transactions on*, vol. 58, no. 9, pp. 4771–4782, 2010.

[10] D. Piazza, J. Kountouriotis, M. D'Amico, and K. Dandekar, "A technique for antenna configuration selection for reconfigurable circular patch arrays," *Wireless Communications, IEEE Transactions on*, vol. 8, no. 3, pp. 1456–1467, 2009.

[11] J. Kountouriotis, D. Piazza, P. Mookiah, M. DAmico, and K. Dandekar, "Reconfigurable antennas and configuration selection methods for MIMO ad hoc networks," *EURASIP Journal on Wireless Communications and Networking*, vol. 2011, no. 1, pp. 1–14, 2011.

[12] R. Blum, "MIMO capacity with interference," *Selected Areas in Communications, IEEE Journal on*, vol. 21, no. 5, pp. 793–801, 2003.

[13] D. Love and R. Heath, "Limited feedback unitary precoding for spatial multiplexing systems," *Information Theory, IEEE Transactions on*, vol. 51, no. 8, pp. 2967–2976, 2005.

[14] N. Gulati, D. Gonzalez, and K. Dandekar, "Learning algorithm for reconfigurable antenna state selection," in *IEEE Radio and Wireless Symposium*. IEEE, 2012.